

## Snap-Through Buckling Problem of Spherical Shell Structure

Sumirin<sup>1</sup>, Nuroji<sup>2</sup> & Sahari Besari<sup>3</sup>

<sup>1</sup>Department of Civil Engineering, Sultan Agung Islamic University, Jl. Raya Kaligawe Km.04, Semarang 50112, Indonesia

<sup>2</sup> Department of Civil Engineering, Diponegoro University, Jl.Prof.Soedarto,SH.Kampus UNDIP Tembalang, Semarang 50275, Indonesia

<sup>3</sup> Department of Civil Engineering, Institute of Technology, Jl. Ganesha 10, Bandung 40132, Indonesia

Email: sumirinms@gmail.com

**Abstract** - This paper presents results of a numerical study on the nonlinear behavior of shells undergoing snap-through instability. This research investigates the problem of snap-through buckling of spherical shells applying nonlinear finite element analysis utilizing ANSYS Program. The shell structure was modeled by axisymmetric thin shell of finite elements. Shells undergoing snap-through buckling meet with significant geometric change of their physical configuration, i.e. enduring large deflections during their deformation process. Therefore snap-through buckling of shells basically is a nonlinear problem. Nonlinear numerical operations need to be applied in their analysis. The problem was solved by a scheme of incremental iterative procedures applying Newton-Raphson method in combination with the known line search as well as the arc-length methods. The effects of thickness and depth variation of the shell is taken care of by considering their geometrical parameter  $\lambda$ . The results of this study reveal that spherical shell structures subjected to pressure loading experience snap-through instability for values of  $\lambda \geq 2.15$ . A form of 'turn-back' of the load-displacement curve took place at load levels prior to the achievement of the critical point. This phenomenon was observed for values of  $\lambda = 5.0$  to  $\lambda = 7.0$ .

**Keywords**— buckling, finite element, snap-through, nonlinear analysis, spherical shell.

Submission: July 3, 2014

Corrected : October 22, 2014

Accepted: December 27, 2014

Doi: [10.12777/ijse.8.1.54-59](https://doi.org/10.12777/ijse.8.1.54-59)

**[How to cite this article:** Sumirin, S., Nuroji, N., and Besar, S. (2015). Snap-Through Buckling Problem of Spherical Shell Structure, *International Journal of Science and Engineering*, Vol. 8(1),54-59. Doi: [10.12777/ijse.8.1.54-59](https://doi.org/10.12777/ijse.8.1.54-59)]

### I. INTRODUCTION

Thin shells is widely used as structural elements in many industrial and construction engineering. Examples of their applications are arch bridges, roof of sport stadiums and convention halls, aircraft parts, industrial components and home appliances, car bodies and so on. One form of shell structures that is widely used in engineering is the shallow spherical shell, i.e. a shell with small arch depth. Such a shell is inexpensive due its small arch length which leads to a small surface and minimal weight. However, it may frequently be found close to its condition of instability.

Buckling is a phenomenon that occurs in slender rods, thin plates and thin shells. Its consequence is essentially a problem of geometry. If large displacements occur, the geometry of the structure changes significantly, bringing with it changes in the method of analysis. Similar events, beside shells, also occur in arch and truss structures (Bazant and Cedolin, 1991).

Snap-through buckling phenomena pose some of the most difficult problems in nonlinear structural analysis (Crisfield,1980). Its occurrence in spherical shell structures has been studied earlier by Karman and Kerr (1962), followed by other researchers such as Bushnell (1989), Uchiyama & Yamada (2000). Load-displacement curve models

representing snap-through buckling of spherical shell structures were described by Karman and Kerr (1962), and Yamaguchi and Chen (1999). Figure 1 shows the basic outline of their curves.

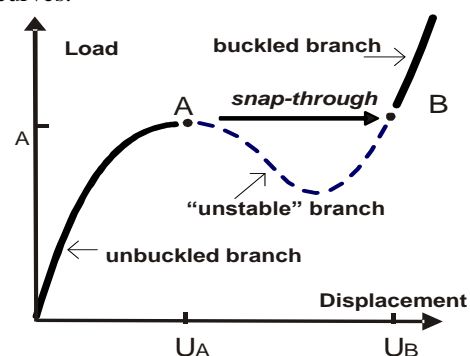


Figure 1. Load-displacement snap-through buckling curve of spherical shell structures (Karman and Kerr, 1962; Yamaguchi and Chen, 1999).

However, experimental results acquired by Kaplan (1954), and Uchiyama and Yamada (2000) showed snap-through curves dissimilar to those shown in Figure 1. The dissimilarity

was later learned due to the difference in the assumed geometrical parameter of the shells.

This study aims to investigate the snap-through buckling problem that occurs in spherical shell structures and examine the effects of variation of their geometrical parameters, shell thicknesses and shell heights on their instability and patterns of snap-through buckling.

## II. MATERIAL AND METHOD

### Description of Model

This study is part of a dissertation research in the Doctoral Program in Civil Engineering Diponegoro University of Semarang, Indonesia. Numerical computational simulation using facility with Finite Element Method ANSYS Program in Design and Tribology Laboratory of the Department of Mechanical Engineering Diponegoro University, Semarang. This research was conducted in 3 months from Februari 2010 to April 2010.

In this research a spherical shell structure like that shown in Figure 2(a) was considered. The structure rests on hinged supports along the rim and is subjected to a uniformly distributed pressure load  $q$ . The shell was then modeled by a number of discrete axially symmetrical elements covering all structural parameters  $h_0$ ,  $R$ ,  $a$ , and  $t$ . Figure 2(b) shows the finite element model of the shell structure. Varying values of  $t$ , ranging from  $0.02a$  to  $0.1a$ , and  $h$ , varying from  $0.05a$  to  $0.5a$  were considered. The shell height may be expressed in terms

of  $R$  and  $a$  as  $h_0 = R - \sqrt{R^2 - a^2}$ . The parameter  $h_0/a$  determines whether the shell is a deep or a shallow one. Kaplan (1954) includes shells with  $h_0/a \leq 1/8$  in the category of shallow shells.

According to the elastic theory, assuming small elastic deformations, critical loads of spherical shells with fixed supports, subjected to uniform pressure, was found to be (Timoshenko and Gere, 1961),

$$q_{cr} = \frac{2 E}{\sqrt{3(1-\nu^2)}} \left( \frac{t}{R} \right)^2 \quad (1)$$

where  $\nu$  is Poisson's ratio,  $E$  is the modulus of elasticity,  $t$  is the shell thickness and  $R$  is the radius of curvature of the shell surface.

Experiments on the buckling of spherical shells were conducted by Kaplan (1954) which acquired experimental critical loads much lower than that given by the classical linear theory of Eq. (1). Kaplan(1954) and then Taeprasartsit and Tao (2005) showed that the behavior of the load-deflection relationship is associated with a geometrical parameter  $\lambda$  of the shell. The parameter was formulated as follows:

$$\lambda = [12(1-\nu^2)]^{1/4} \frac{a}{\sqrt{R} t} \quad (2)$$

where  $a$  is the radius of the horizontal base of shell.

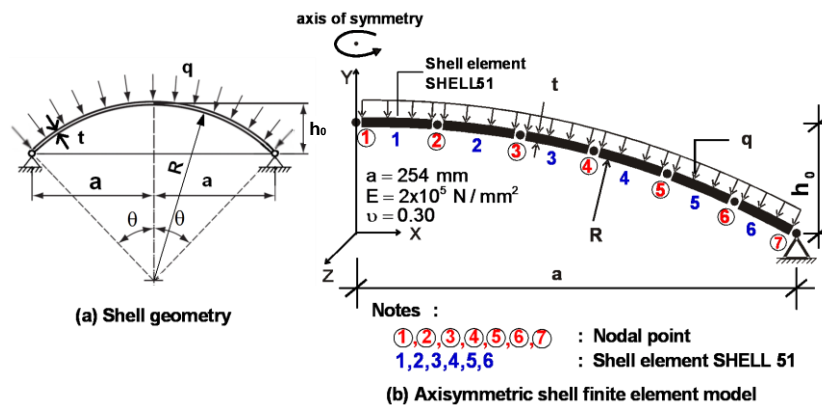


Figure 2. Shell structure geometry and its finite element model

### The Geometric Nonlinear Finite Element Analysis Methods

Snap-through buckling is a geometric nonlinear problem of which the solution can be approximated by nonlinear finite element analysis. In such analysis, the considered equilibrium condition is the one prevailing at the last structural configuration. The element stiffness matrix and the load vector are derived applying the *updated Lagrangian* formulation. The procedure has been comprehensively described by Bathe (1982) and ANSYS (2009).

The equilibrium equation at the  $i$ -th iteration of the  $n$ -th loading stage is,

$$[K_i^T] \{\Delta u_i\} = \Psi \{F^a\} - \{F_i^{nr}\} \quad (3)$$

where  $[K_i^T]$  is the tangent stiffness matrix,  $i$  and  $n$  are subscripts indicating the  $i$ -th iteration and the  $n$ -th load step,  $\{F_i^{nr}\}$  is the restoring load vector depending on the element forces or stresses and  $\Psi$  is the load level parameter. In general the value of  $\Psi$  varies between  $-1 \leq \Psi \leq 1$ .  $[K_i^T]$  and  $\{F_i^{nr}\}$  are evaluated based on the given value of displacement  $\{\Delta u_i\}$ . The right-hand side of Equation (3) represents the out-of-balance residual force vector. Iterations carried out at each load increment are implemented in a similar manner. The procedure is illustrated on Figure 3(a) (ANSYS, 2009).

The application of the constant arch-length method was necessary in recognizing critical points and the generation of the downward branch of a snap-through load-displacement curve beyond its critical point. The method was developed by Crisfield based on a method previously described by Wempner and Risk (Crisfield, 1980; Boediono, 1995).

Newton-Raphson's method still functions as the basis of the constant arch-length approach. The approach is illustrated in Figure 3(b). The non-linear equation of the method may be written as (Crisfield, 1980; ANSYS, 2009),

$$[K_i^T] \{\Delta u_i\} = \Psi \{F^a\} - \{F_i^{nr}\} \quad (4)$$

At the n-th load sub-step and i-th iteration, the following equation may be written,

$$[K_i^T] \{\Delta u_i\} - \Delta \Psi \{F^a\} = (\psi_n + \psi_i) \{F^a\} - \{F_i^{nr}\} = -\{R_i\} \quad (5)$$

where  $\Delta \Psi$  represents the incremental load parameter.

The displacement increment  $\{\Delta u_i\}$  consists of two parts:

$$\{\Delta u_i\} = \Delta \Psi \{\Delta u_i^I\} + \{\Delta u_i^{II}\} \quad (6)$$

where  $\{\Delta u_i^I\}$  is the displacement due to a unit load increment and  $\{\Delta u_i^{II}\}$  is the displacement increment due to Newton-Raphson's method, where:

$$\{\Delta u_i^I\} = [K_i^T]^{-1} \{F^a\} \quad (7)$$

$$\{\Delta u_i^{II}\} = -[K_i^T]^{-1} \{R_i\} \quad (8)$$

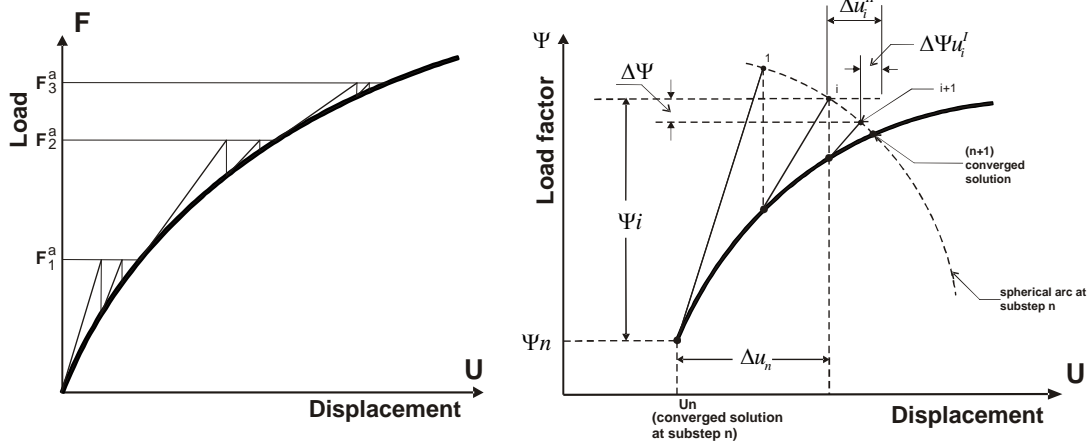
At each iteration the arc length method utilizes Equations (7) and (8) to obtain the values of  $\{\Delta u_i^I\}$  and  $\{\Delta u_i^{II}\}$ . The load level increments  $\Delta \Psi$  are obtained from the arch-length equation of the i-th iteration as follows,

$$\ell_i^2 = \psi_i^2 + \beta^2 \{\Delta u_n\} \{\Delta u_n\}^T \{\Delta u_n\} \quad (9)$$

where  $\beta$  is a scale factor (having displacement units), and  $\ell_i$  is the radius of the arc length (in the force scale). Equation (6) and (9) are used to calculate the solution vector  $(\Delta u_i, \Delta \Psi)^T$ . Load level increment  $\Delta \Psi$  can be calculated by:

$$\Delta \Psi = \frac{r_i - \{\Delta u_n\}^T \{\Delta u_i^{II}\}}{\beta^2 \psi_i + \{\Delta u_n\}^T \{\Delta u_i^{II}\}} \quad (10)$$

where  $r_i$  is a scalar for explicit iteration on a sphere is first calculation.



(a) The Newton-Raphson's method. (b) The arc-length method.  
Figure 3. Load increments of Newton-Raphson's method and arc-length approach (ANSYS, 2009)

### Axially Symmetric Shell Element Model

The shell elements used in this study were axially symmetrical shell elements which have the ability to endure large deflection and represent stress stiffening effects. This kind of element is available in the ANSYS Program as SHELL51 (ANSYS, 2009). Stress stiffening effect accounts for the operation of membrane forces which is responsible of the buckling of shells. SHELL51 element possesses two nodal points with four degrees of freedom each, i.e. the translational nodal displacements in the X, Y, and Z directions and a rotational about the Z axis. These displacements are sequentially denoted by  $U_x, U_y, U_z$  and  $\theta_z$ , as shown in Figure 4. The validity of applying element SHELL51 in the analysis was corroborated by analysis results applying nonlinear elastic quadrilateral shell elements SHELL63 which contains 4 nodal points.

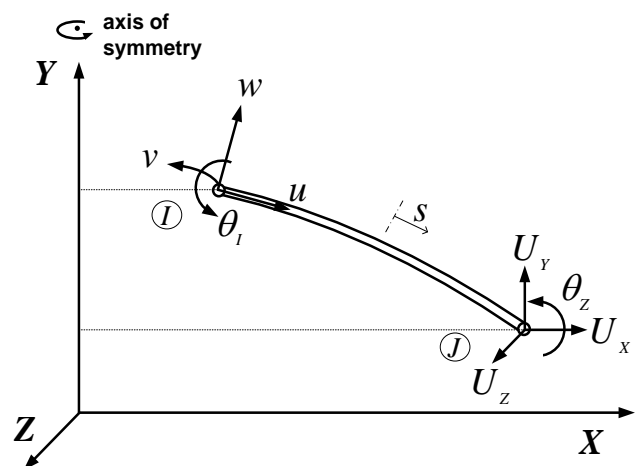


Figure 4. Notation of nodal degrees of freedom of axially symmetric shell element SHELL51.

### III. RESULTS AND DISCUSSIONS

#### Snap-Through Buckling Behavior

Analysis results of a nonlinear shell with geometric parameters  $\lambda=3.0$ , height  $h_0=12.7$  mm, radius of curvature  $R=2346$  mm, thickness  $t=9.303$  mm are incorporated in the load-displacement curve shown on Figure 5. Stability was maintained along path 0-1. Upon the attainment of the critical point, the displacement of the apex point remains  $U_{0y} < h_0$ . The deformed shape of the shell is still convex. An equilibrium condition at an infinitesimal load increase above the critical load in the neighborhood of point 1 was not found. The following equilibrium condition for loads above the critical point was found along the curve branch 3-4. This branch was reached by a large sudden jump in deflection. This jump is described by the curve 1-3, which actually is representing the buckling phenomenon. The downward branch of the load-displacement curve beyond the critical point was obtained by applying the constant arch-length approach.

The displacements of the apex point proceed along the rotational axis of symmetry of the shell. At point 2 the deflection of the apex point has exceeded  $h$ . After buckling the shell assumes a downward concave shape. Beyond, but adjacent to, the critical point 1, equilibrium conditions can only be obtained by applying load reductions or adding negative charges in the analysis. After point 2 displacements increase with increasing loads. The curve eventually will reach point 3 and point 4 and beyond. The displacement of the apex point  $U_{y0}$  has now exceeds the value of  $h_0$  and the shell has a downward concave geometry.

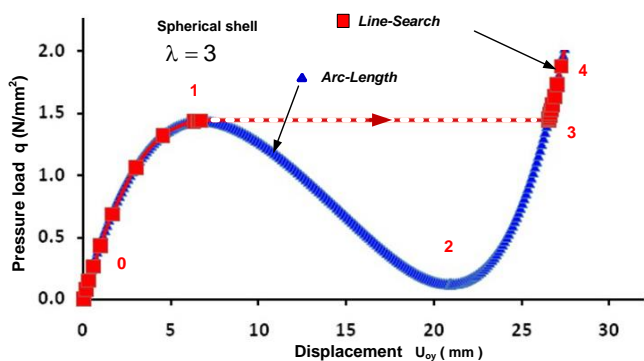


Figure 5. Load-displacement curve a spherical shell with  $\lambda = 3.0$ .

The arch length method as well as the line search method was used as the solution techniques in this study. Both methods are founded on the basic Newton- Raphson approach. The arch-length method performs very well in generating undulating curves like that taking place in cases of snap-through buckling. However this method requires previously determined favorable estimates of load increments and arch radii to warrant the attainment of critical points through convergent iterations. Line search is advantageous due to its accelerating iteration process, but unfortunately, it is not capable of converging to points on a downward progressing curve. Therefore these two methods are used to complement each other in generating the load-displacement curves. In difficult situations, like that around critical points, the combined use of both methods may help accelerate the

iteration process as previously proposed by Crisfield (1980) and later applied by Boediono (1995).

At values of  $\lambda < 4.0$ , applying 25 load steps with arch radius of 1, the process converges quickly to the desired points. However, at values of  $\lambda \leq 4.0$ , tedious adjustments by trial and error need to be done on the values of load stages and arch radii.

#### Comparative Study of Shell Element Type

A study was conducted on the validity of the use of axisymmetric shell element SHELL51 by comparing the results with those where other types of elements were applied. For this purpose trapezoidal elements SHELL63 were considered. These elements were applied on a spherical shell having the following data,  $\lambda=3.0$ ,  $h=12.7$ mm,  $t=9.303$ mm,  $\nu=0.3$ , and  $E=2 \times 10^5$  N/mm<sup>2</sup>. The shell was hinged supported along its rim. Mesh patterns with 12x6, 24x6, 48x6, and 72x6 elements were reviewed.

The results are compiled in Figure 6 Curve (1) represents the results of the shell with 12x6 element mesh. The curve shows significant deviations. While the other four curves, inclusive Curve (5) obtained from 6 Elements SHELL51 mesh, approximately coincide with each other. This excellent coincidence demonstrates the efficiency of Element SHELL63 due to the small number of elements required to model the shell.

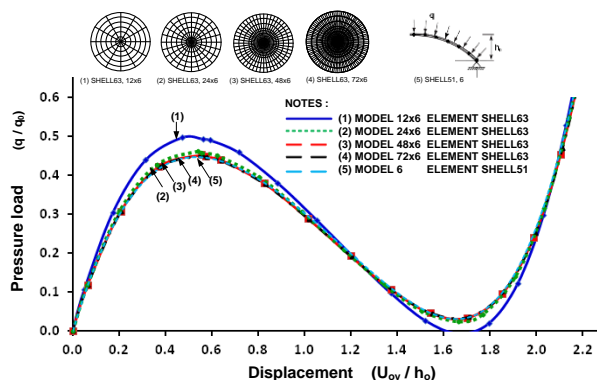


Figure 6. Load-displacement curves of  $\lambda = 3.0$  with four different mesh pattern of element SHELL51 and one with 6 elements SHELL63

#### Comparison with Kaplan's Results

Kaplan (1954) conducted experiments on a number of shallow spherical shells with base diameter  $a=8$  inches, radius of shell curvature  $R=20$  inches and 30 inches, and varying shell thickness and shell height. The specimens were made of aluminum-magnesium alloy QQ-M-44 having an elastic modulus  $E=6.5 \times 10$  psi and Poisson's ratio  $\nu=0.32$ . The pressure load was generated by a hydraulic pressure pump and was raised by a 20 psi capacity Bourdon tube. Deflections were measured using dial-gages with accuracy of 0.001 inches. The results of these experiments were much referenced by subsequent researches, in particular Fung and Sechler (1974), and Uchiyama and Yamada(2000).

In this research a comparative study was made between Kaplan's (1954) experimental results with those obtained from finite element analyses where axially symmetric elements SHELL51 were used. Comparison could be made with the first three specimens tested by Kaplan, namely

Specimens #1, #2, and #3, since test data and numerical finite difference analyses are available. Figure 7 shows Kaplan's test results as well as his finite difference analysis. The figure shows that Kaplan's test results are significantly lower than his polynomial load-displacement model. It also shows that the results of finite element analysis applying element SHELL51 correlates better with Kaplan's analysis rather than with his test results. Many researchers attributed this deficiency to the intrinsic imperfection of test specimens.

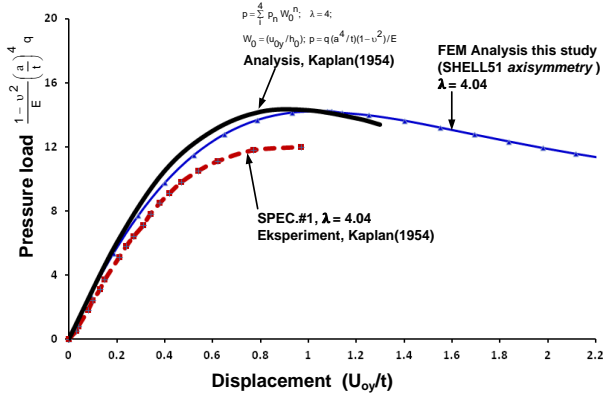


Figure 7. Comparison of load-displacement curves obtained by Finite Element Analysis with Kaplan's experimental work for Spec#1.

Effect of Thickness, Radius of Curvature, and Geometric Parameter  $\lambda$

In Figure 8 and Figure 9 are presented load-displacement curves of spherical shells with varying  $\lambda=0.0$  to  $\lambda=9.0$ . Figure 8 shows that buckling does not take place in shells with  $\lambda=0.0$  and  $\lambda=2.0$ . Snap through does occur in shells with  $\lambda \geq 2.5$ . Figure 9(a) shows load-displacement curves of shells with  $\lambda=4.0, 5.0, 6.0,$  and  $7.0$ . These shells produce curves having close resemblance with each other, i.e. they possess a sharp critical point before continuing downward with increasing displacements. These curves, however, differ significantly with those exhibited by shells with  $\lambda=2.5,$  and  $3.0$  (Figure 8). Shells with  $\lambda=5.0, \lambda=6.0,$  and  $\lambda=7.0$  reveal a peculiar 'turn-back' phenomenon, i.e. prior to reaching their critical points the deflections of the apex point reverts (turn back up) with

increasing loads. This feature was not reported by previous researchers (Felippa, 2004; Uchiyama and Yamada, 2000; Kaplan, 1954). However, having the same features with those of curves of  $\lambda=5.0, 6.0,$  and  $7.0,$  Shells with  $\lambda=4.0$  does not exhibit the surprising turn-back phenomenon.

The deformation history of Figure 8 shows that the buckling mode of shells with  $\lambda=2.5$  and  $\lambda=3.0$  proceeded in a global manner, i.e. the shell configuration changes drastically in one instance from a convex shape into a concave one. Contrary, the buckling of shells with  $\lambda=5.0, \lambda=6.0, 7.0, 8.0,$  and  $9.0$  proceeded in a composite manner. The global snap-through is preceded by a local buckling. This event is clarified by the deformation history shown in Figures 9(a) and 9(b). The deformation history of Figure 9(a) shows that prior to the attainment of the concave shape, the shell experienced local buckling at the rim. This explains the turn-back phenomenon referred to earlier. The local buckling deflection at the shell edge pushes the apex up. The deformation history shown on Figure 9(b) demonstrates that prior to the attainment of concave configuration the shell experienced local buckling at the apex.

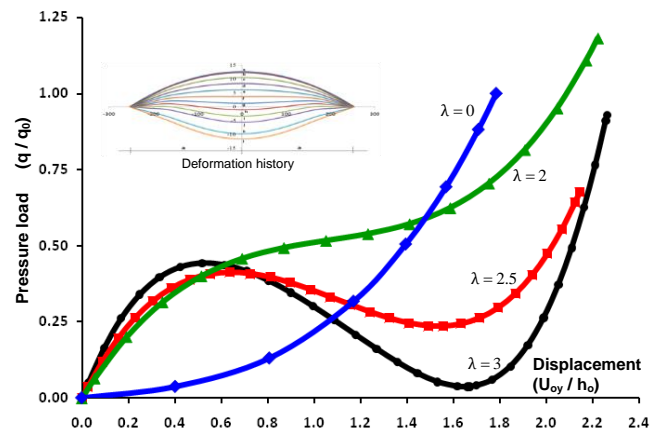


Figure 8. Load-displacement curve of nondimensional shell structure,  $\lambda=0$  to  $\lambda=3.0$ .

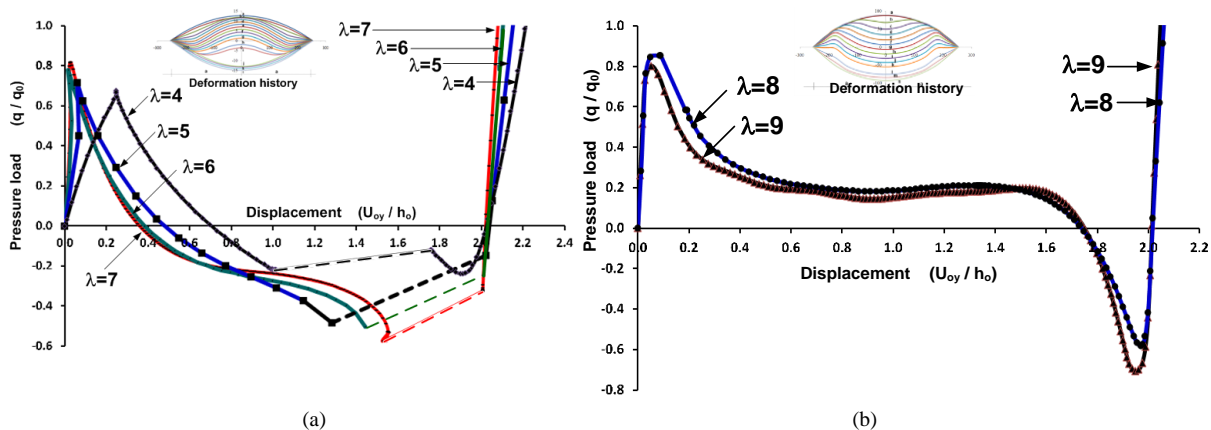


Figure 9. (a) Load-displacement curve of Shells with  $\lambda=4, \lambda=5, \lambda=6,$  and  $\lambda=7$ ; (b) Load-displacement curve of Shells with  $\lambda=8$  and  $\lambda=9.0$ .

The load-displacement curve of shells with  $\lambda=2.5,$  shown in Figure 8, indicates that snap-through takes place at the critical point, while buckling does not occur in shells with

$\lambda=2.0$ . Somewhere in between there is a transition point where the shell turns from a stable shell into an instable one. By more refined analysis, with two digits accuracy, this point

was found to be  $\lambda=2.15$ . Shells with  $\lambda \geq 2.15$  will experience snap-through buckling at their critical load. Kaplan (1954) contended that instability occurs in shells with  $2 < \lambda < 3$ .

To comprehend the effects of shell thickness  $t$ , curvature radius  $R$ , and parameter  $\lambda$ , on the behavior of spherical shells, it is necessary to look into their interrelations. For that purpose the chart in Figure 10 was constructed. It illustrates the relation of  $t/a$  and  $R/a$ , where  $a$  is the radius of the base circle of the shell and  $\lambda$  is a geometric parameter. The transition curve  $\lambda=2.15$  is also shown. Points 1 to 9 drawn on the transition curve indicate shells with differing thickness and curvature, but of the same value  $\lambda=2.15$ . All these differing shells are transition shells. Numerical checks have shown these shells behaves in a similar manner with respect to instability. They produce exactly the same load-deflection curves. Shells represented by curves on the right hand side of the transition curve  $\lambda=2.15$  are stable. At sufficiently large loads, these shells exhibit a deformed shape similar to that of a buckled shell. However, the configuration takes shape through a smooth continuous process, not a sudden event of snap-through. Shells represented by curves at the left hand side of the transition curve are subject to snap-through instability. Figure 10 shows that for  $t/a \leq 0.05$  the value of  $\lambda$  is very sensitive to changes in shell thickness. The chart on this Figure may be put to practical use in determining the stability of spherical shells.

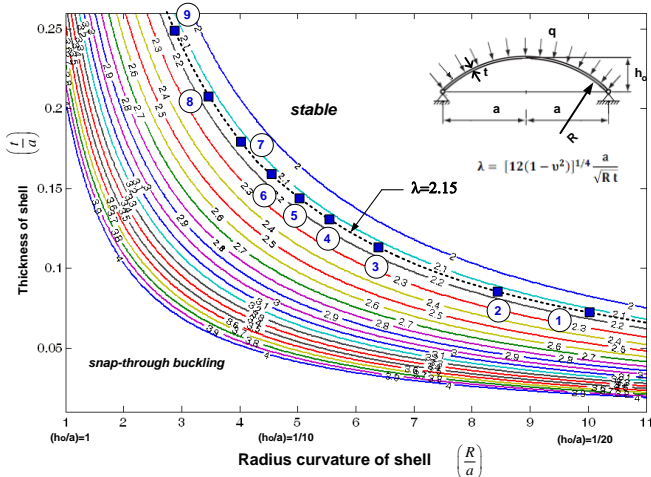


Figure 10. Inter-relation of  $(t/a)$ ,  $(R/a)$  and  $\lambda$  with transition curve of  $\lambda=2.15$  of spherical shell.

#### IV. CONCLUSIONS

- Shells with  $\lambda=2.15$  are transition shells. Shells with  $\lambda < 2.15$  are stable, while those with  $\lambda \leq 2.15$  are subject to snap-through instability.
- At sufficiently large loads, stable shells exhibits a deformed shape similar to that of a buckled shell, however, it proceeds in a smooth transition manner, not a sudden event of snap-through.
- Shells with  $2.15 \leq \lambda \leq 3.0$  buckles globally in a single instance.
- The global snap-through of shells with  $\lambda=4.0$ ,  $\lambda=5.0$ ,  $6.0$ , and  $7.0$  is preceded by local buckling along the shell edge.

- The global snap-through of shells with  $\lambda=8.0$  and  $9.0$  is preceded by local buckling at the apex of the shell.
- The transition point between the case of single instance global buckling of shells with  $\lambda \leq 3.0$  and that preceded by local buckling at the edge of shells with  $\lambda=4.0$ ,  $\lambda=5.0$ ,  $6.0$ , and  $7.0$  lies in the interval of  $3.0 < \lambda < 5.0$ .
- The transition point of the case of global buckling preceded by local buckling at the edge of shells with  $\lambda \leq 7.0$  and that preceded by local buckling at the apex of shells with  $\lambda \geq 8.0$  lies in the interval of  $7.0 < \lambda < 8.0$ .
- Shells with  $\lambda=5.0$ ,  $6.0$ , and  $7.0$  exhibit a 'turn-back' phenomenon prior to snap-through.
- Shell analysis applying element axisymmetric SHELL51 of ANSYS is more efficient than using trapezoidal element SHELL63 due to the small number required to model the shell.

#### ACKNOWLEDGEMENTS

The authors are greatly indebted to the head and staff of the Department of Mechanical Engineering, Diponegoro University, for their assistance and the use of their ANSYS Program.

#### REFERENCES

- ANSYS. 2009. Theory Reference for the Mechanical APDL and Mechanical Applications, Release 12.1, ANSYS, Inc. South Pointe 275 Technology Drive, Canonsburg.
- Bathe, K.J. 1982. Finite Element Procedures in Engineering Analysis. Prentice-Hall, New Jersey.
- Bazant, Z.P. and Cedolin, L. 1991. Stability of Structures, Oxford University Press, New York Oxford.
- Budiono, R.B. 1995. Hysteretic Behaviour of Partially-Prestressed Concrete Beam-Column Connections. Thesis of Doctor of Philosophy, Department of Structural Engineering School of Civil Engineering, University of New South Wales.
- Bushnell, D. 1989. Computerized Buckling Analysis of Shells. Kluwer Academic Publishers. The Netherlands.
- Chen, W.F., dan Lui, E.M. 1987. Structural Stability. Elsevier Science Publishing Co., Inc. New York.
- Crisfield, M.A. 1980. A Fast Incremental Iterative Solution Procedure that Handles Snap-Through, Computer and Structures, Vol.13 pp.55-62, England.
- Felippa, C.A. 2004. Advanced Finite Element Methods. Department of Aerospace Engineering Sciences, University of Colorado at Boulder, <http://caswww.colorado.edu/courses/d/AFEM.d/Home.html>
- Fung, Y.C., and Sechler, E.E. 1974). Thin Shell Structures, Prentice-Hall Inc., Englewood Clift, New Jersey, U.S.A.
- Kaplan, A. 1954. Finite Deflection and Bending of Curved and Shallow Spherical Shells under Lateral Loads, Thesis Doctor of Philosophy, California Institute of Technology Pasadena, California.
- Karman, V.T., dan Kerr, A.D. 1962. Instability of Spherical Shells Subjected to External Pressure, National Aeronautics and Space Administration, Washington.
- Taepasartsit, S. and Tao, K. 2005. Effect of Shell Geometry and Material Constant on Dynamic Buckling Load of Elastic Perfect Clamped Spherical Caps, Asian Journal of Civil Engineering (Building and Housing), Japan, Vol.6, No.4, pp.303-315.
- Uchiyama, M. and Yamada, S. 2000. Nonlinear Buckling Simulations of Imperfect Shell Domes using a Hybrid Finite Element Formulation and the Agreement with Experiments, Fourth International Colloquium on Computation of Shell & Spatial Structures, Chania-Crete, Greece.
- Yamaguchi, E. and Chen, W-F. 1999. Basic Theory of Plates and Elastic Stability, Structural Engineering Handbook, Boca Raton, CRC Press LLC.